Xiangtang Downhole Array of Accelerometers-Instrumentation and Observation

LI Shabai , ZHANG Wenbo and XIE Li-Li

Institute of Engineering Mechanics, State Seismological Bureau of China
9, Xuefu Road, Harbin 150080, P. R. China

Synopsis

The Xiangtang downhole array (XTDA) for the effects of local site conditions on strong ground motion is a three-element array of three-component, force balance accelerometers for measuring accelerations up to 2.0 g over a frequency range from 0 to 50 Hz. The accelerometers are placed at depths of 0 m, 16 m and 32 m respectively. The lithostratigraphy is about 12 m of soil overlying a 18 m layer of strong weathered granulite and granite below which is moderate-weathered granite. The array is located at the intersection of the Taoyuan fault and the Leting fault, it is only 18 km from the epicenter of the largest aftershock (Ms=7.1, July 28, 1976) of Tangshan earthquake (Ms=7.8, July 28, 1976). An M_L =5~6 earthquake would be expected in the near future in this area. From its installation in September 1994 through December 1995, it recorded 27 local earthquakes with magnitudes ranging from 1.7 to 5.9. The maximum acceleration recorded at the soil surface is 60.1 cm/s/s from an M_L =5.9 earthquake. The surface to downhole spectral ratios show that there are significant differences in the frequency contents between the soil surface and the underground rock measuring points. The surface deposits at XTDA site have two resonance frequencies, around 4.4 Hz and 8.8 Hz, where the spectral ratio amplitudes are more than 10, for horizontal ground motions. Amplifications of the surface soil layer exist up to 50 Hz. In contrast to the weathered granite layer (16-32 m), the surface soil deposits (0-16 m) play more important role in amplifications of ground motion.

Key Words: surface soil deposit, acceleration, ground motion, magnitude, frequency

1. Introduction

It is well known that the local geological condition has been proved to play an important role in the earthquake ground motion. The effects of the local geological condition include: the effects of amplification and attenuation on ground motion, sand liquefaction and the slide caused by earthquakes. In the present, the model of soft soil overlying hard rock has been accepted by many engineers, and this site condition has two contrary effects on the earthquake ground motion: on one hand, due to the difference between two materials and their impedance, the effect of free surface and the resonance of soil, the earthquake ground motion will be amplified; on the other hand, because of the existence of the quality factor Q of mediums, it will be attenuated (Shearer, et al., 1987 and Arculeta, et al., 1992).

In order to quantify the relative contributions of these factors on amplification and attenuation of earthquake ground motion, and select the reasonable baserock motion as the input of the soil response, it must establish special downhole arrays to obtain the real data of surface ground motion and underground motion simultaneously. It is necessary to verify the reliability and effectiveness of the existing calculation

model and method, and give the better calculation model and method by analyzing the obtained data.

The purpose of the Xiangtang downhole array is to obtain the accelerograms of stiff soil and underground rock, and use these data to verify and compare the model and method of this type site condition. That is to say, Xiangtang Downhole Array (XTDA) is an observation array that directly measures the effects of the local geological conditions on the amplification and attenuation of seismic wave (Xie and Li, 1992).

2. Location and Geological Condition of the XTDA Array

ground motion; Second, the geological condition should have enough effects on ground motion, ad these effects can be measured by instrument; Third, the site should be typical, its topographic and geomorphologic features are relatively simple, it should be similar with the sites for municipal and industrial engineering; Last, it should have a good transport service. These criteria are satisfied at Xiangtang, Hebei Province, China.

Xiangtang is in a seismic area. The well known two earthquakes occurred in this area: Tangshan earthquake (Ms=7.8, July 28, 1976) and its largest aftershock (Ms=7.1, July 28, 1976). Aftershocks

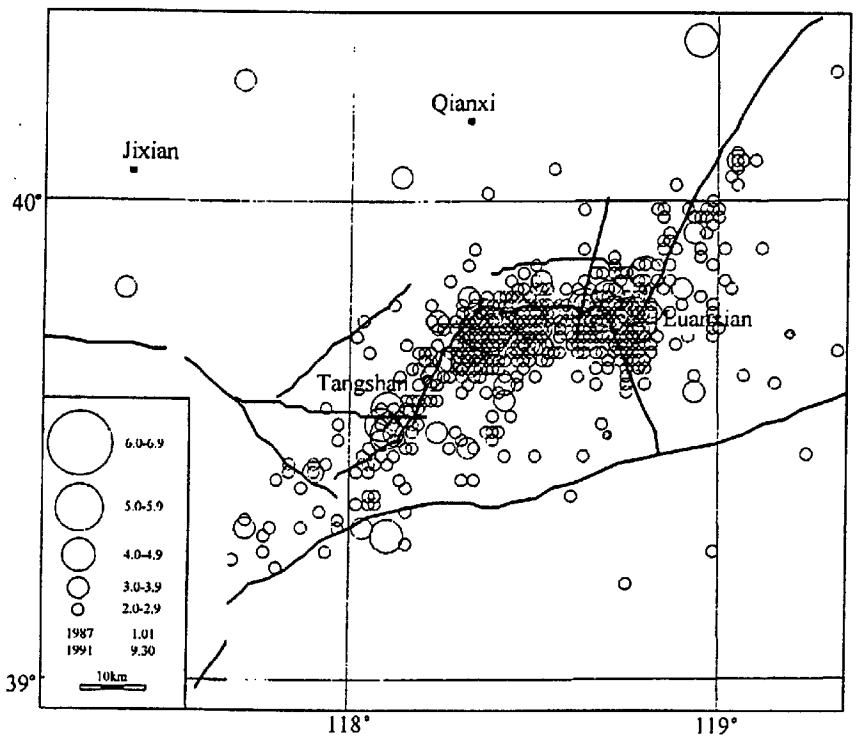

Fig. 1 The distribution of aftershock of Tangshan earthquake occurred from 1987 to 1991

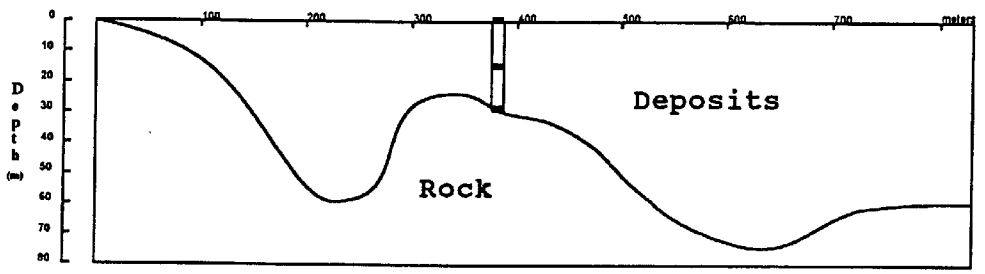

Fig. 2 Section of Xiangtang Downhole Array

The site of XTDA was selected in mind with several basic criteria. First, it should be in a seismic active area that would produce both strong and weak

occur frequently in this area. Figure 1 is the distribution of aftershocks of Tangshan earthquake occurred from 1987 to 1991. In there years, there

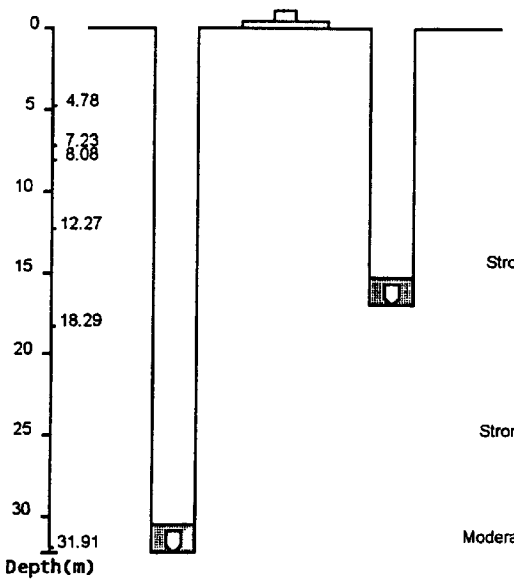

Fig. 3 Location of the sensors

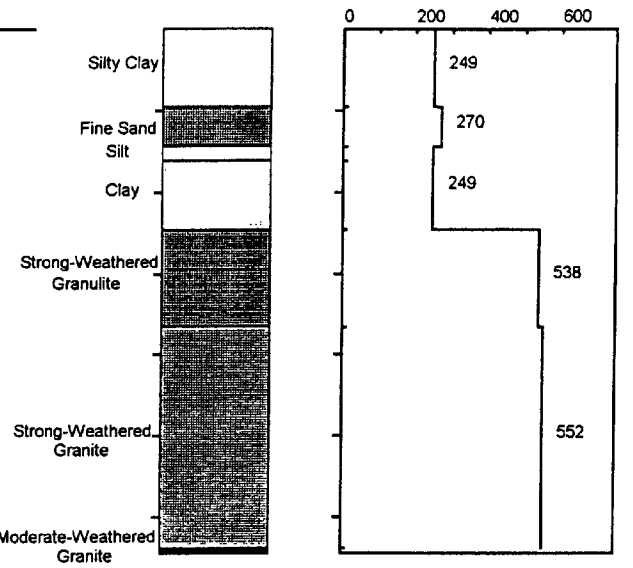

Fig. 4 Earthquake structure and S-wave velocity (m/s) in downhole

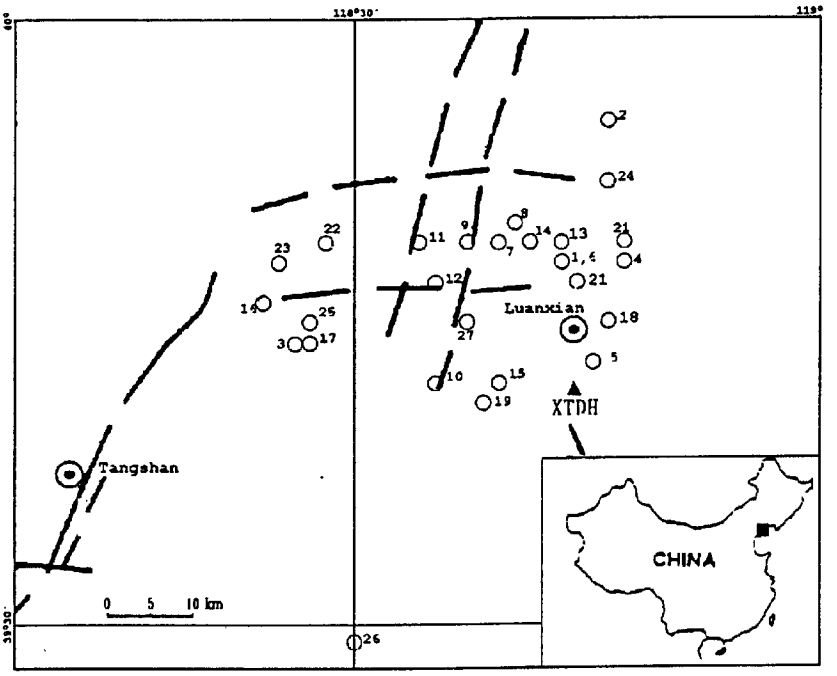

Fig. 5 Map showing epicenters of the 27 earthquakes listed in Table 1

were two or three M=4 earthquakes every year in this area. An M=5-6 earthquake would be expected in the near future in this area. In Xiangtang, the maximum thickness of soil layer is less than 100 meters and the relative elevation is less than 40 m. So, Xiangtang is selected as the array site for the effects of local geological conditions on seismic ground motion. The array is situated at the intersection of the Taoyuan and Leting fault, it is only 18 km from the epicenter of the largest aftershock (Ms=7.1, July 28, 1976) of Tangshan earthquake (Ms=7.8, July 28, 1976).

XTDA was developed in July 1994. Before that, S-wave velocity structure of its site was assumed. Detailed description of the site characteristics as follows: XTDA is located in southwest of Duyu village, Xiangtang (39:41.7′N, 118:44.03′E). The

soil column at the site consists of 4.78 m of silt clay, 2.45 m of fine sand, 0.85 m of silt clay, 4.19 m of clay, 6.02 m of strong-weathered granulite, 13.62 m of strong-weathered granite and 0.40 m of moderate-weathered granite. There are two drill holes (A&B) for measuring ground motion. The depth hole A is about 32 m and its tilt is less than 36′, and the depth of hole B is about 16 m and its tilt is less than 30′. Figure 2 is the section of underground rock in Xiangtang area. Figure 3 is the location of the sensors in XTDA and Fig. 4 is lithology and the S-wave velocity structure at XTDA.

3. Instrumentation

At the free surface soil, 0 m, three FBA-11 force balance accelerometers are installed. At the underground measuring points (16 m and 32 m), FBA-13DH downhole triaxial accelerometer packages (full scale: 2g) are deployed. Recorder used at measuring points 0 m, 16 m and 32 m are two SSR-1 solid state recorders. One has six channels as the master unit by which ground motion signals from measuring points 0 m and 32 m are recorded. The other has three channels as slave unit by which ground motion signals from 16 m measuring point are recorded. The master unit is always responsible for generating the system scan clock and the system functional test signal, synchronizing the time code and triggering the system.

The recorder of SSR-1 is the key instrument in XTDA, it is a highly flexible digital seismic event recorder with solid-state RAM. It can support up to six sensors, and sample rate can be set up to 200 sps for 6 channels. The SSR-1 utilizes a 16 bit A to D converter to provide 90 dB of dynamic range. To

Table 1 Earthquake Parameters

Event	Trigging Time	M_L	ϕ_N	λ_E	Depth (km)	Δ (km)	Azimuth
01	09/30/94-19:01:14.515	2.4	39°48′	118°43′	5	11.8	353°
02	10/02/94-03/08:25.470	3.6	39°55′	118°46′	5	24.8	7°
03	10/04/94-15:54:26.384	4.0	39°44′	118°26′	11	26.1	279°
04	10/24/94-17:05:47.334	3.3	39°48′	118°47′	--	12.4	20°
05	10/24/94-17:28:05.884	2.5	39°43′	118°45′	--	2.8	31°
06	12/17/94-06:15:40.000	2.7	39°48′	118°43′	--	11.8	353°
07	12/29/94-13:12:10.000	2.1	39°49′	118°39′	--	15.3	332°
08	01/08/95-20:33:54.339	2.3	39°50′	118°40′	--	16.4	340°
09	01/11/95-12:40:06.840	2.3	39°49′	118°37′	5	16.8	324°
10	02/07/95-01:51:53.540	2.7	39°42′	118°35′	--	12.9	272°
11	03/02/95-07:47:06040′	2.7	39°49′	118°34′	--	19.7	314°
12	03/30/95-19:39:51.760	2.2	39°47′	118°35′	12	16.1	307°
13	05/06/95-05:09:47.080	2.3	39°49′	118°43′	--	13.6	354°
14	05/13/95-17:21:00.580	1.7	39°49′	118°41′	--	14.2	342°
15	05/20/95-06:47:03.358	2.0	39°42′	118°39′	--	7.4	274°
16	06/23/95-14:21:02.855	3.5	39°46′	118°24′	--	29.6	286°
17	06/27/95-22:46:18.600	3.0	39°44′	118°27′	13	24.7	280°
18	07/02/95-15:19:40.985	2.9	39°45′	118°46′	13	6.9	25°
19	07/05/95-19:20:53.985	2.3	39°41′	118°38′	--	8.6	279°
20	08/31/95-19:27:48.190	2.4	39°49′	118°47′	--	14.3	18°
21	09/13/95-16:15:51.110	2.2	39°47′	118°44′	--	9.6	0°
22	09/19/95-23:48:11.110	2.9	39°49′	118°28′	10	26.5	301°
23	09/20/95-00:25:54.110	3.8	39°48′	118°25′	5	29.5	293°
24	10/03/95-14:57:22.110	2.9	39°52′	118°46′	14	19.4	8°
25	10/06/95-06:27:00.610	5.9	39°45′	118°27′	--	25.0	284°
26	12/17/95-07:35:07.420	2.8	39°29′	118°30′	7	30.9	320°
27	12/31/95-00:08:53.420	3.0	39°45′	118°37′	--	11.7	302°

increase sensitivity, a 60 dB pre-amp is selected in 20 dB a step. Triggering can be accomplished in four different modes: external, ratio of STA vs. LTA, difference of STA vs. LTA, bandpass filtered threshold, and pre-programmed time frames called experiment windows.

For a high quality array, it must have a highly accurate timing system. The SSR-1 has a Timing System board that provides the SSR-1 with a millisecond resolution system clock, a synchronized scan clock, and alarm wake-up capacity, also controls the optional Omega board. For XTDA, it selects the Omega board to update the Timing System clock, it receives the Omega navigation signal which is transmitted from Japan.

The downhole accelerometer packages were lowered into the boreholes using a set of loading poles with square shape section. Before and after installing the packages, the offsets of the accelerometers were checked to assure that the offsets were less than 5 mv and the packages were located in the local vertical position. The orientation of the horizontal components can be roughly estimated by means of a loading pole which has a red mark on its side. Following Aster and Shearer (1991a), and using the variance tensor method, we fit an ellipse to the first cycle of P wave arrival particle motions projected on the horizontal plane. If we assume that the semi-major axis of the ellipse aligns with the backazimuth of an event, orientation of the horizontal component accelerometer can be obtained. We select 3 sets of horizontal accelerometer of event 16, event 23 and event 25 in which the first P arrival motions are recorded with high signal-to-noise ratio and the first cycle of P arrival particle motions are nearly linearly polarized (linearity > 0.9). Results show that orientation of horizontal component accelerometers at 32 m are constant with that at 0 m, and orientation difference between 0 m and 32 m is about 2°, and 11° of the difference exists between 0 m and 16 m.

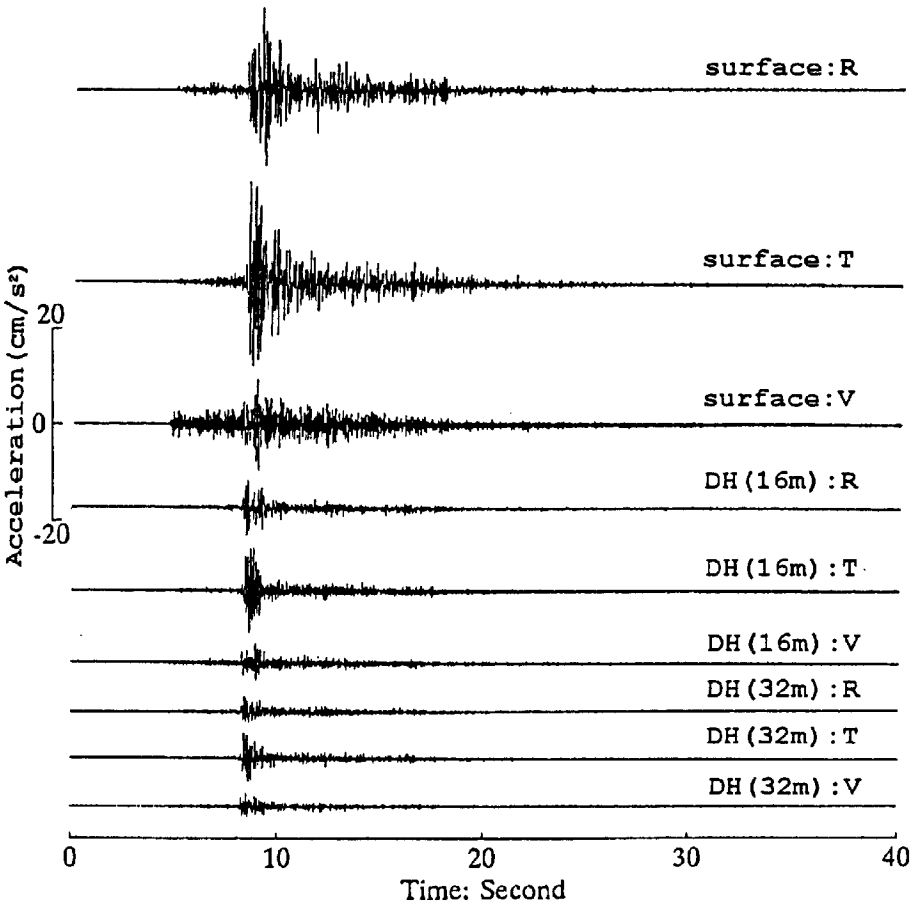

Fig. 6 Accelerograms generated by the Event 03, M_L=4.0, October 4, 1994; Parameters of the earthquake are: origin time: 10/04/1994, 15:54:17.2 BT; focal depth: 11 km; epicenter location: 39° 44'N, 118° 26'E; epicenter distance: 26 km; backazimuth 279°.

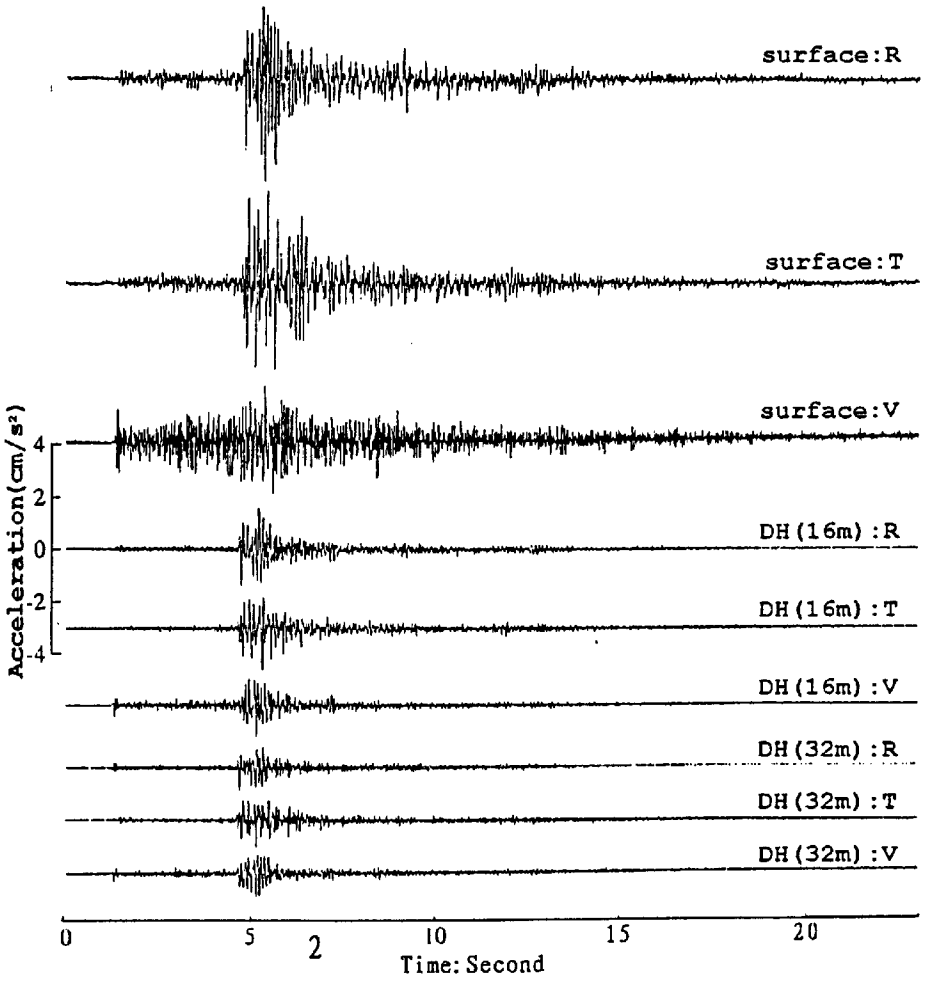

Fig. 7 Accelerograms generated by the Event 17, M_L=3.0, June 27, 1995; Parameters of the earthquake are: origin time: 06/27/1995, 22:46:18.6 BT; focal depth: 13 km; epicenter location: 39° 44'N, 118° 27'E; epicenter distance: 24.7 km; backazimuth 280°.

4. Data and Analysis Methods

From September 1994 through December 1995, 27 local earthquakes ranging in magnitudes from 1.7 to 5.9 and epicentral distance from 2 to 31 km were recorded at the XTDA array. The XTDA array location and epicenters of the 27 earthquakes are plotted in Fig. 5. Earthquake parameters from the seismic monthly catalogs of Institute of Geophysics, SSB, are listed in Table 1. The maximum acceleration is 60.1 cm/s/s on the vertical component at the surface (event 25, M_L=5.9, $\triangle$=25 km).

The recorded accelerograms have entire phases, clear wave forms, accurate timing and higher signal-to-noise ratio. As examples, three component accelerograms obtained at 0 m, 16 m, and 32 m from event 3 and event 17 are shown in Figs. 6 and 7. In these figures, two horizontal components are rotated into the radial and transverse component based on the event backazimuths.

We select 12 sets of accelerograms from 27 earthquakes to carry out spectral ratio analysis. The parameters of the 12 earthquakes are also listed in Table 1. The 12 earthquakes are divided into two groups based on the event backazimuths. One group, including event 3, 16, 17, 22, 23 and 25, are located in the west of the XTDA. Their backazimuths are from 279° to 301°; The other group, including event 13, 14, 18, 20, 21 and 24, are located in the north of the XTDA. Corresponding backazimuths are from -18° to 18°. The accelerograms at each depth generated by the 12 earthquakes have high signal-to-noise ratio. As an example, Fig. 8 provides the acceleration Fourier amplitude spectra of signal and noise calculated from accelerograms of event 3 recorded at 0 m and 32 m, respectively. It can be seen from Fig. 8 that there are high signal-to-noise ratios in frequency range of 0.3 to 50 Hz and noise levels at 32 m is about 20 dB lower than that at 0 m.

To examine more closely the amplification of each depth as a function of frequency, ground motion

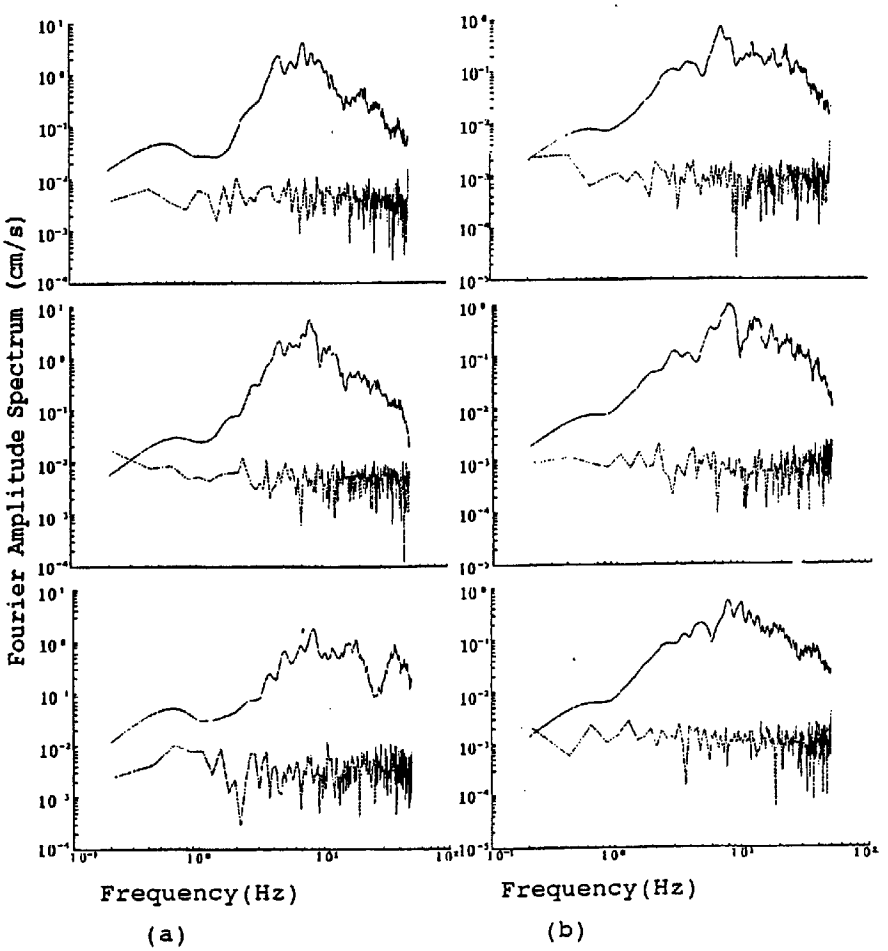

Fig. 8 Fourier amplitude spectra of Event 03, M_L=4.0, Oct. 4, 1994; (a) surface; (b) downhole; From the top to the bottom is the component of R, T, and V respectively; Solid line is the spectra of signal and dash line is the spectra of noise.

amplification, expressed as the spectral ratio 0/16, spectral ratio 16/32 and spectral ratio 0/32, has been calculated for the 3 orthogonal components (radial, transverse and vertical) using entire accelerograms. For a meaningful comparison of spectral ratio from different earthquakes, some conventions are used in spectral calculations. The horizontal components are rotated into the radial and transverse component based on the event backazimuths; Calculation length of an accelerogram is 25 seconds and corresponding spectral resolution is 0.04 Hz; Acceleration amplitude spectra are smoothed using a Hanning window whose with is 1 Hz; Before spectral calculation, the offset of an accelerogram is estimated using the pre-event noise and is subtracted it from the accelerogram.

5. Spectral Ratio Results

The surface to downhole spectral ratio can significantly reduce the variability due to source and path differences (Aster et al., 1991), and can provide partial information on how ground motion are amplified by sediment deposits (Liu et al., 1992).

The spectral ratios of 3-component acceleration amplitude spectra, including 0/16, 16/32 and 0/32, generated from event 3 and event 17 are shown in Figs. 9a and 9b, respectively. It is clear from Fig. 9 that amplification effects of the surface sediment deposits are dependent on frequency contents of ground motions. The spectral ratios 0/16 and 0/32 have gross similar shapes. This shows that the surface soil layer play an important role in the ground motion amplifications and most modification to the seismic waves occurs in the uppermost 16 m. In contrast, the spectral ratios 16/32 are relatively flat. The relative flatness of the spectral ratios 16/32 is also reflected in the time domain by similar waveforms recorded at 16 m and 32 m from the same event (Figs. 6 and 7). As shown in Fig. 9, the spectral ratios 0/16 and 0/32 are generally greater than unit in frequency band, f<50 Hz. This fact indicates that amplifications of the surface soil layer (0-16 m) are pronounced due to the effects of free surface, impedance contrast amplification, converted phase and resonance, although the soil layer has low quality factor, Q. Figures 9a and 9b also show that the

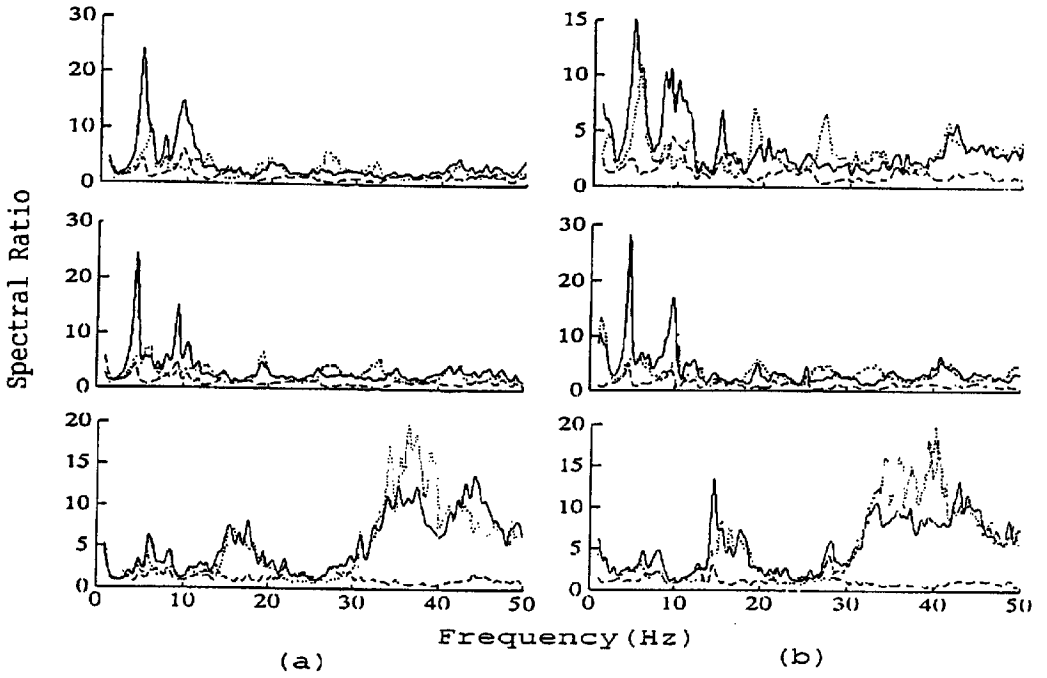

Fig 9 Spectral ratio: (a) Event 03, M_L=4.0, Oct. 4, 1994; (b) Event 17, M_L=3.0, Jun. 27, 1995; From the top to the bottom is the component of R, T, and V respectively; Solid line is 0m/32m, dash line is 16m/32m, and dot line is 0m/16m.

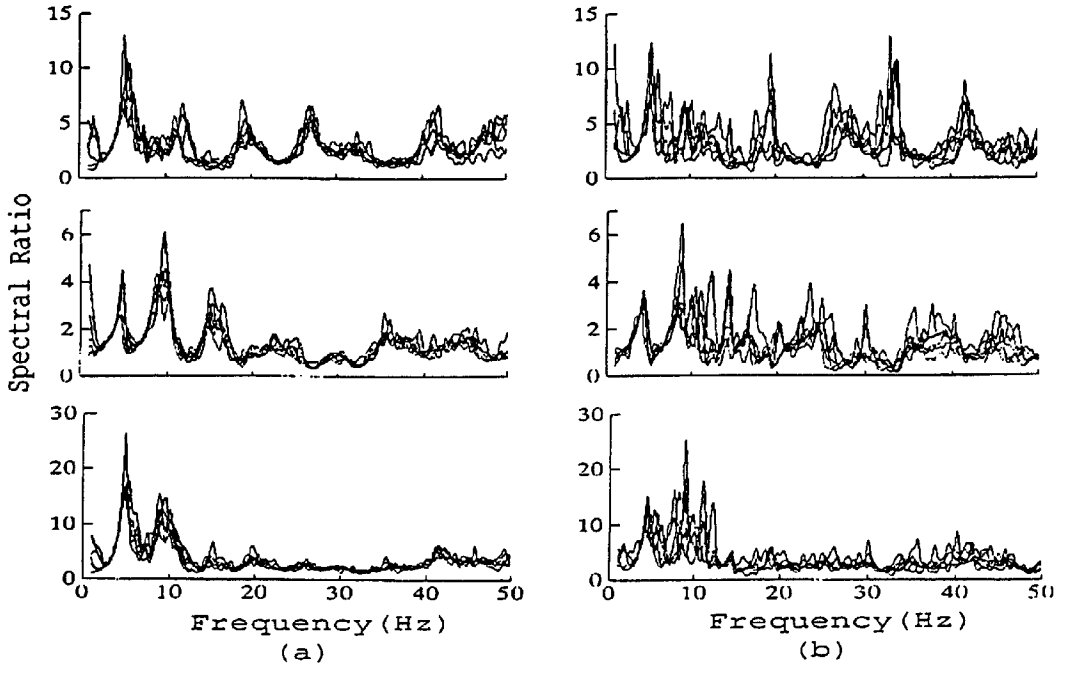

Fig. 10 Stacked spectral ratio (component R): (a) group one including Event 03, 16, 17, 22, 23, 25; (b) Group two including Event 13, 14, 18, 20, 21, 24. From the top to the bottom is the spectral ratio of 0m/16m, 16m/32m, and 0m/32m respectively

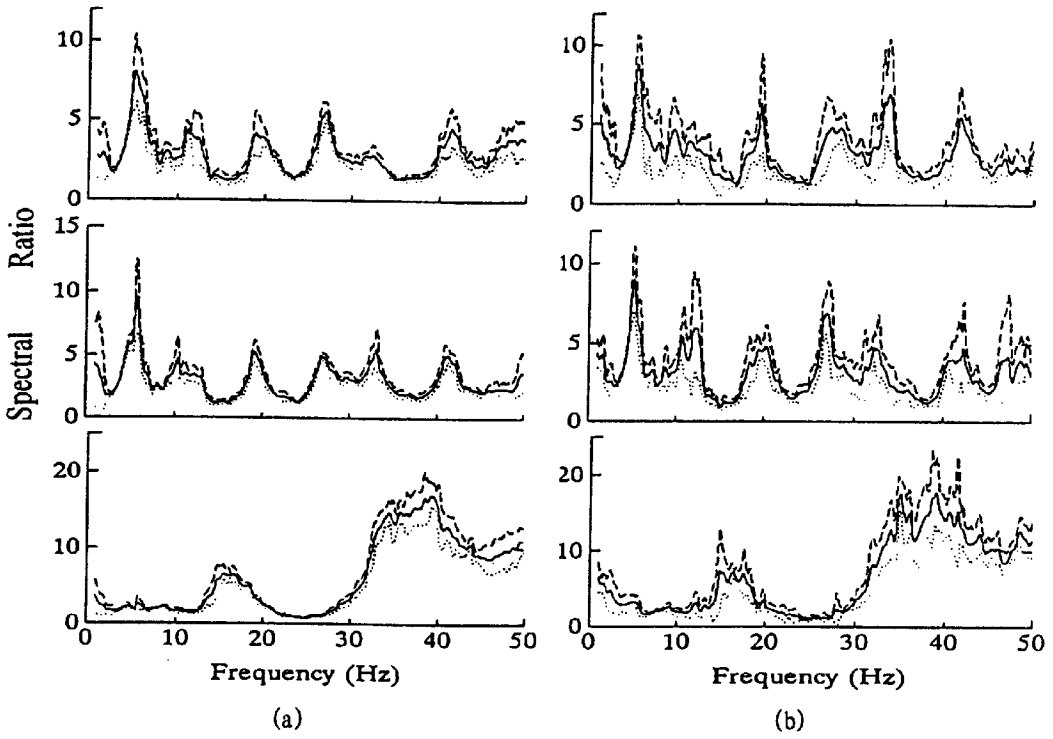

Fig. 11 The mean spectral ratio of 0m/16m: (a) Group one including Event 03, 16, 17, 22, 23, 25; (b) Group two including Event 13, 14, 18, 20,21, 24. From the top to the bottom is the component R, T and V respectively

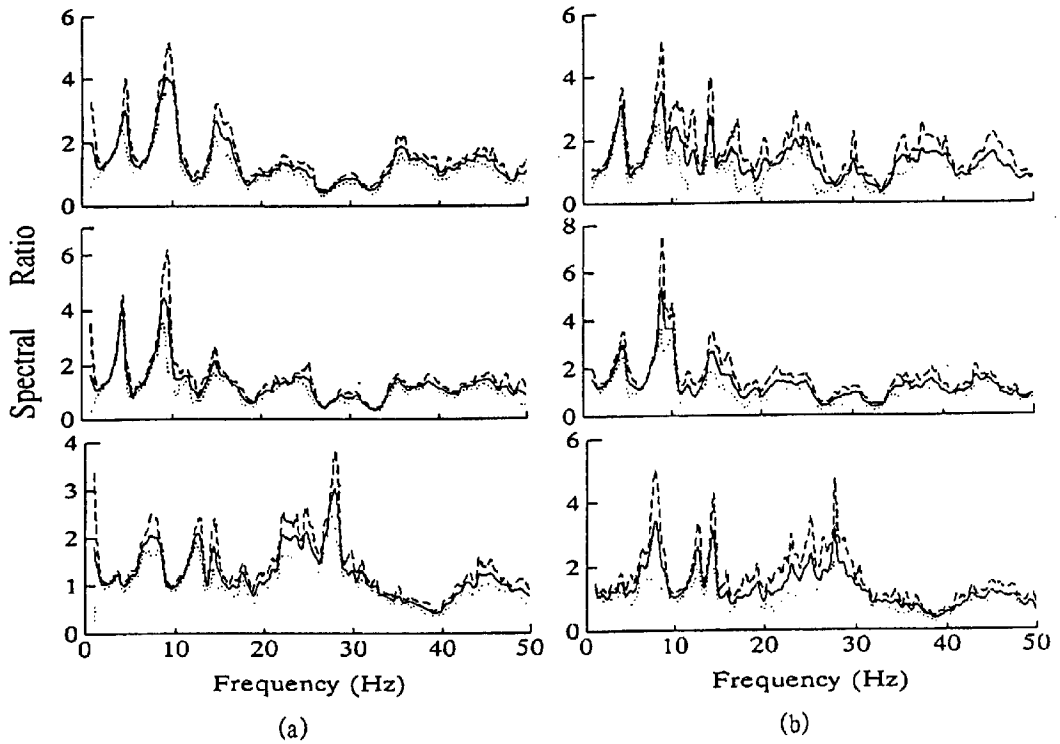

Fig. 12 The mean spectral ratio of 16m/32m: (a) Group one including Event 03, 16, 17, 22, 23, 25; (b) Group two including Event 13, 14, 18, 20,21, 24. From the top to the bottom is the component R, T and V respectively

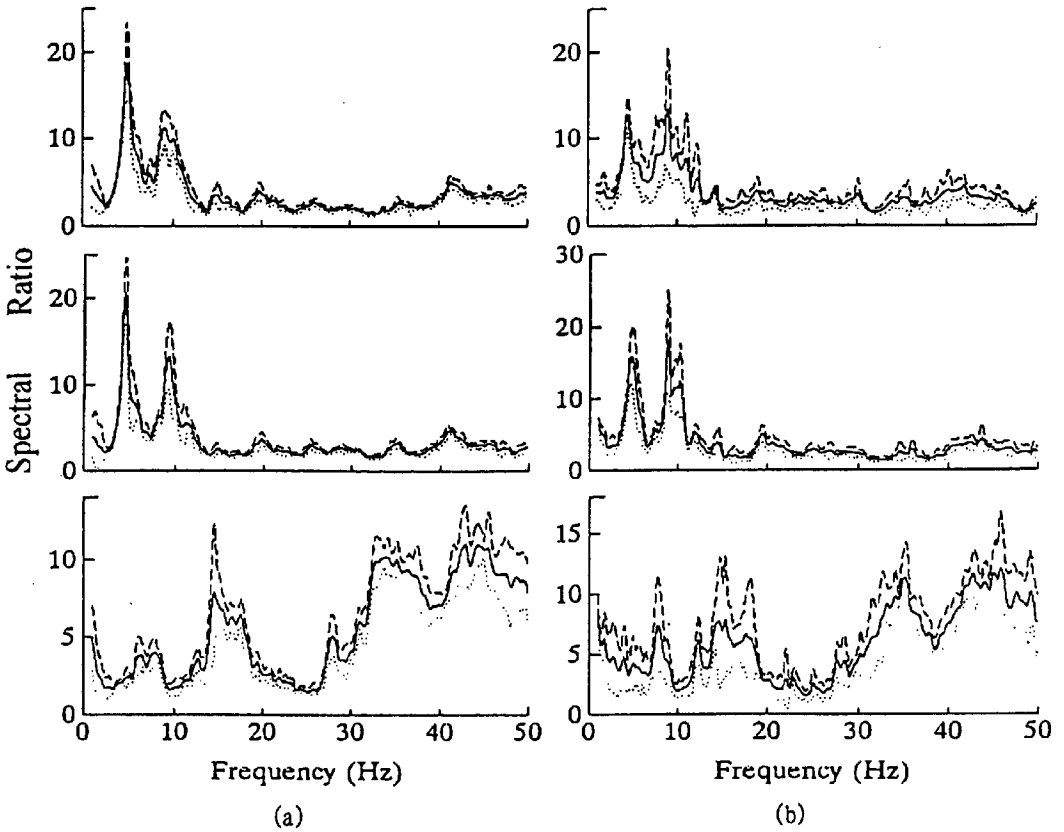

Fig. 13 The mean spectral ratio of 0m/32m: (a) Group one including Event 03, 16, 17, 22, 23, 25; (b) Group two including Event 13, 14, 18, 20,21, 24. From the top to the bottom is the component R, T and V respectively

spectral ratios of two horizontal components have similar characters and the spectral ratio peaks occur in frequency band, f<15 Hz. There are obvious differences between the vertical and horizontal spectral ratios. The soil layer (0-16 m) amplifies, evidently, the vertical ground motions in high frequency band (35 to 50 Hz).

To estimate the effects of the XTDA site on ground motion, the spectral ratios 0/16, 16/32 and 0/32 for the "West group" and the "North group" earthquakes are overlaid in a plotting, first. The spectral ratios of radial component at each depth for the "West group" and "North group" earthquakes are stacked in Figs. 10a and 10b, respectively. It is shown that these spectral ratios for each group have good coherence, although the coherence for the "North group" is less than that for the "West group". Figure 10 also shows that it is effective to adopt the spectral ratio method in describing the effects of the surface deposits on ground motion. Next, average spectral ratios for each group earthquakes are given. Figures 11, 12 and 13 provide the average spectral ratios of 3 components at each depth for the "West group" and "North Group" earthquakes, respectively. In these figures, mean and $\pm\sigma$ bounds are represented by solid, dashed and dotted traces, respectively. The average spectral ratios indicate clearly that the surface deposits at XTDA site (0-32 m) mainly amplify the ground motions of horizontal components in a low frequency band (f<15 Hz) and two frequency peaks exist in the frequency band (Fig. 11 to Fig. 14). For the "West group" earthquakes, the frequency peaks are at 4.7 Hz, 8.9 Hz (radial comp.), and 4.4Hz, 9.1Hz (transverse comp.), and amplitudes of the frequency peaks are 18.8, 11.3 (radial comp.) and 20.7, 13.3 (transverse comp.), respectively. For the "North group" earthquakes, the frequency peaks are at 4.2 Hz, 8.8 Hz (radial Comp.), and 4.6, 8.7 Hz (transverse Comp.), and amplitudes of the frequency peaks are 12.8, 13.4 (radial Comp.) and 16.0, 18.2 (transverse Comp.), respectively. This shows that amplitudes of spectral ratio peaks have variation depending on ground motion direction and earthquake location. This observation is consistent with that obtained at a downhole array in the Marina district of San Francisco (Liu, et al., 1992). The spectral ratio amplitudes at the frequency peaks more than 10 indicate that resonances occur and the frequency peaks correspond the resonance frequencies of the XTDA site. Amplification of the vertical component is complicated. There are stronger amplifications for the vertical component in

a frequency band from 15 Hz to 20 Hz, and an unusual amplifications exist around 35 Hz and 45 Hz, which would be analyzed further. Comparing the average spectral ratios 0/16, 16/32 and 0/32, it is clear that amplification of the surface soil layer (0-16 m) is much stronger than that of the weathered granite layer (16-32 m).

6. Summary

The Xiangtang array is the first observation station that is directly measuring the effects of local site conditions on seismic ground motion in China. The digital acceleration recording system install at XTDA array is capable of measuring accelerations up to 2.0 g over a frequency ranges from 0 Hz to 50 Hz. Since its full operation in September 1994, the array has recorded more than 27 earthquakes with magnitudes from 1.7 to 5.9 and epicentral distances from 2 km to 31 km. The maximum acceleration is 60.1 cm/s/s on the vertical component obtained from event 25 at the surface. The recorded accelerograms have high signal-to-noise ratio and entire phases. The spectral ratio analysis show that the surface soil layer has a pronounced effects on ground motion amplification in the frequency band from 0 to 50 Hz, and the resonance peaks exist at about 4.4 Hz and 8.8 Hz for horizontal components, and amplification of the spectral ratio peaks vary from 11 to 21. The spectral ratios from the 12 earthquakes give an indication of the variation in spectral ratio to be expected from earthquakes with magnitudes, $1.7 < M_L < 5.9$ and epicentral distances, $2 < \Delta < 31$ km in the Tangshan-Xiangtang area.

The analysis presented here is preliminary. The purpose of this report has been to illustrate the quality of the XTDA array data and give the observation facts.

References

ARCHULETA, R. J., SEALE, S. H., SANGAS, P. V., BAKER, L. M. and SWAIN, S. T. (1992): Garner valley downhole array of accelerometers: instrumentation and preliminary dada analysis, *BSSA 82*, No. 4, pp. 1592-1621.

ASTER, R. C. and SHEARER, P. M. (1991a): High-frequency borehole seismograms recorded in the San Jacinto fault zone, southern California, part 1: polarization, *BSSA 81*, No. 4, pp. 1057-1080.

ASTER, R. C. and SHEARER, P. M. (1991b): High-frequency borehole seismograms recorded in the San Jacinto fault zone, southern California, part 2: attenuation and site effects, *BSSA 81*, No. 4, pp. 1081-1100.

LIU, H. P., WARRICK, R. E., WESTERLUND, R. E., SEMBERA, E. D. and WENNERBERG, L. (1992): Observation of local site effects at a downhole and surface station in the Marina district of San Francisco, *BSSA 82*, No. 4, pp. 1536-1591.

SHEARER, P. M. and ORCUTT, J. A. (1987): Surface and near-surface effects on seismic waves-theory and borehole seismometer results, *BSSA 77*, No. 4, pp. 1168-1196.

XIE, L. L. and LI, S. B. (1992): An experimental array at Tangshan for the effects of surface geology on seismic motion, *Proc. of workshop on China-Japan joint research for earthquake disaster prediction and mitigation*, Beijing, China.

要旨

局所的なサイト特性が強震動に与える影響を検討するために，ボアホール地震観測システムが唐山市 Xiangtang 地域に構築された。地表，地下-16m 及び地下-32m に 3 成分加速度型強震計が設置された。観測可能最大地動加速度及び周波数範囲は，それぞれ，±2g 及び 0～50 Hz である。これまでに，27 個の局所地震が観測された。これらのマグニチュード（M）は 1.7～5.9 の範囲であった。また，これまでに観測された最大加速度は，M=5.9 の地震時の 60.1 cm/s/s である。地表/地下の地動振幅スペクトル比の解析から，この地域の表層地盤の共振周波数は 4.4 及び 8.8 Hz あたりにあることがわかった。

キーワード：ボアホール地震観測，加速度記録，地震動，増幅率，共振周波数，活断層